

Measurements of hydroperoxy radicals (HO₂) at atmospheric concentrations using bromide chemical ionization mass spectrometry

Sascha R. Albrecht¹, Anna Novelli¹, Andreas Hofzumahaus¹, Sungah Kang¹, Yare Baker¹, Thomas Mentel¹, Andreas Wahner¹, and Hendrik Fuchs¹

¹Forschungszentrum Jülich GmbH, Institute of Energy and Climate Research, Troposphere (IEK-8), 52428 Jülich, Germany

Correspondence: Sascha Albrecht (s.albrecht@fz-juelich.de)

Abstract.

Hydroxyl and hydroperoxy radicals are key species for the understanding of atmospheric oxidation processes. Their measurement is challenging due to their high reactivity, therefore very sensitive detection methods are needed. Within this study, the measurement of hydroperoxy radicals (HO₂) using chemical ionization combined with an high resolution time of flight mass spectrometer (Aerodyne Research Inc.) employing bromide as primary ion is presented. The sensitivity reached is equal to 0.005 × 10⁸ HO₂ per cm³ for 10⁶ cps of bromide and 60 s of integration time, which is below typical HO₂ concentrations found in the atmosphere. The detection sensitivity of the instrument is affected by the presence of water vapor. Therefore, a water vapor dependent calibration factor that decreases approximately by a factor of 2 if the water vapor mixing ratio increases from 0.1 to 1.0 % needs to be applied. An instrumental background most likely generated by the ion source that is equivalent to a HO₂ concentration of $(1.5 \pm 0.2) \times 10^8$ molecules cm⁻³ is subtracted to derive atmospheric HO₂ concentrations. This background can be determined by overflowing the inlet with zero air. Several experiments were performed in the atmospheric simulation chamber SAPHIR at the Forschungszentrum Jülich to test the instrument performance by comparison to the well-established laser-induced fluorescence (LIF) technique for measurements of HO₂. A high linear correlation coefficient of $R^2 = 0.87$ is achieved. The slope of the linear regression of 1.07 demonstrates the good absolute agreement of both measurements. Chemical conditions during experiments allowed testing the instrument's behavior in the presence of atmospheric concentrations of H₂O, NO_x and O₃. No significant interferences from these species were observed. All these facts are demonstrating a reliable measurement of HO₂ by the chemical ionization mass spectrometer presented.

Copyright statement.

1 Introduction

Understanding of the oxidation processes in the atmosphere requires sensitive measurements of the radical species involved. Hydroxyl radicals (OH) are the most important oxidative species and are highly reactive to most of the inorganic and organic

pollutants in the atmosphere. Primary sources of OH radicals are mainly ozone photolysis and in polluted environments also nitrous acid (HONO) photolysis can be of importance. Organic pollutants are oxidized by OH to produce organic peroxy radical species (RO₂) and also hydroperoxy radicals (HO₂). OH and HO₂ radicals are closely inter-connected by a radical chain reaction, in which OH is reformed by the reaction of HO₂ with nitric oxide (NO):



As the atmospheric lifetime of HO₂ radicals is typically up to a factor 10 longer than that of OH radicals, HO₂ can be regarded as an important chemical reservoir for hydroxyl radical (OH). Atmospheric NO concentrations are often sufficiently high to maintain an efficient OH production by the reaction of HO₂ with NO, so that Reaction R1 provides a large portion of the total OH production. Measurements of both species are needed to analyze the OH radicals budget.

10 The majority of the techniques currently applied to measure atmospheric concentrations of HO₂ radicals use chemical conversion, which is an indirect measurement. In chemical amplifying systems, a radical reaction cycle between OH and HO₂ is established by adding two reactants. The concentration of the product species is therefore amplified compared to the small, initial HO₂ concentration in the sampled air.

PERoxy RadiCal Amplification (PERCA) instruments make use of NO and CO for the conversion of HO₂ to OH and OH to HO₂, respectively. One NO₂ molecule is produced in each reaction cycle so that the initially small HO₂ concentration is amplified as NO₂, which is then detected by a luminol detector, fluorescence or absorption methods. Because RO₂ is also converted to HO₂ in the reaction with NO, these instruments measure the sum of RO₂ and HO₂. Typically an amplification of roughly a factor of 100 is achieved to produce a measurable amount of NO₂ (Cantrell et al., 1984; Hastie et al., 1991; Clemittshaw et al., 1997; Burkert et al., 2001; Wood et al., 2017; Sadanaga et al., 2004; Mihele and Hastie, 2000; Green et al., 2006; Andrés-Hernández et al., 2010).

Alternatively to CO, SO₂ can be used in the chemical amplifier system (Reiner et al., 1997; Hanke et al., 2002; Edwards et al., 2003; Hornbrook et al., 2011). The high sensitivity of CIMS measurement using nitrate (NO₃⁻) as primary ion allows to detect sulfuric acid (H₂SO₄) produced in the reaction of SO₂ with OH. Amplification factors of approximately 10 are sufficient in this case. Like in the PERCA instrument, RO₂ is also converted to HO₂ in the reaction with NO in these instruments. 25 However, Hornbrook et al. (2011) developed a method to distinguish between HO₂ and RO₂ by operating the instrument at different chemical conditions (varying NO, SO₂ and O₂ concentrations) thereby changing the relative sensitivities for HO₂ and RO₂.

Laser-induced fluorescence (LIF) is a sensitive technique for OH radical measurements and it is used for the indirect detection of HO₂ by its conversion into OH after reaction with NO. The concurrent conversion of some specific RO₂ radicals can contribute to the HO₂ signal (Fuchs et al., 2011; Whalley et al., 2013; Lew et al., 2018). This can be minimized by reducing the NO concentration added to the sampled air for the conversion of HO₂ to OH, but on the cost of a reduced sensitivity. A comparison of three LIF instruments in 2010 before the RO₂ interference was discovered showed significant differences in 30

measured HO₂ concentration in experiments in the SAPHIR chamber (Fuchs et al., 2010). This could have been partly due to interferences from RO₂, but measurements also differed depending on the water vapor concentration.

Several drawbacks are connected with existing HO₂ detection methods. The PERCA systems exhibit a strong water vapor dependence of the amplification factor. In addition, chemical conversion of HO₂ by the reaction with NO used in all instruments
5 can lead to the concurrent conversion of RO₂.

Previous work by Veres et al. (2015) showed that HO₂ radicals can be detected with a CIMS instrument using iodide as primary ion. Sanchez et al. (2016) demonstrated for the first time that this approach can also be used with Br⁻. HO₂ radicals are directly measured by a mass spectrometer as an ion cluster formed with bromide ions. Sanchez et al. (2016) demonstrated that the most promising ionization technique is the detection of the bromide cluster with HO₂. In their work they showed
10 that a sufficient sensitivity for atmospheric measurements can be achieved and no significant interference from NO_x, HCHO, SO₂, O₃ is present. Following the concept of Sanchez et al. (2016) a bromide chemical ionization mass spectrometer with improved sensitivity was developed in this work. An optimized ionization flow tube was custom built and mounted on top of a commercial, high resolution time-of-flight mass spectrometer (TOF-MS, Aerodyne Res.). In addition to laboratory characterization experiments that mostly confirmed results reported in Sanchez et al. (2016), the performance of the instrument was
15 quantitatively assessed in a comparison of HO₂ concentrations with measurements by an established HO₂ instrument using laser-induced fluorescence. Experiments in the atmospheric simulation chamber SAPHIR were performed at atmospheric gas mixtures and radical concentrations.

2 Methods

2.1 Chemical ionization mass spectrometry technique

20 The instrument used for the detection of the Br⁻ · HO₂ cluster consists of a custom-built ion flow tube (Fig. 1) that is mounted upstream of a TOF-MS. For the detection of reactive HO₂ radicals, losses in inlets can play a significant role. As radical species are easily lost by contact on walls, the inlet of the instrument is designed to sample air directly into the ion flow tube without additional inlet lines. The TOF-MS is equipped with an atmospheric pressure ionization (APi) transfer stage providing the ion transfer from the ion flow tube to the detector. The TOF mass analyzer (Tofwerk AG, Switzerland) has a mass resolution better
25 than 2000.

Ambient air containing HO₂ (flow rate 3.4 slm; slm = liters at standard conditions, T = 0 C and p = 1013 hPa) is sampled through a 0.7 mm skimmer nozzle and is mixed with the bromide ions in the ion flow tube shown in Fig. 1. The ion flow tube has an inner diameter of 22 mm and a length of 130 mm. The distance between the ion source and the nozzle downstream is 100 mm. The ion flow tube is kept at a constant pressure of 120 hPa using a butterfly control valve upstream of a scroll pump.
30 Assuming that 5.4 slm of gas are passing through the ion flow tube the mean residence time is 240 ms assuming plug-flow conditions. Longer versions of the ion flow tube of up to twice its size were tested, but a reduced sensitivity for HO₂ was found. Downstream of the ion flow tube, the sampled air enters a commercially available transfer stage (CI-API transfer stage,

Aerodyne Research Inc.) through a nozzle with 0.5 mm diameter. The transfer stage consists of two quadrupoles and direct current transfer optics that guide the ions to the TOF analyzer. Laboratory experiments were performed at 25 to 30 ° Celsius.

Bromide ions easily clusters with polar species e.g. acids (Caldwell et al., 1989). This enables their detection in the gas phase including HO₂, which is a relative strong acid (the binding energy is 353 kcal mol⁻¹ Harrison (1992)). In order to produce Br⁻ ions, a gas flow of 2 slm nitrogen is mixed with 10 sccm of a 0.4 % mixture of CF₃Br in nitrogen (Air Liquide Deutschland GmbH, N₂ 99.9999 % purity). The resulting gas mixture of approximately 20 ppmv CF₃Br in nitrogen is supplied to the 370 MBq ²¹⁰Po ion source (Type P-2021-5000, NDR Static Control LLC, USA) to generate bromide ions, resulting in an ion count rate of 1 × 10⁵ cps.

The isotopic pattern of bromide (approx. 1 ⁷⁹Br : 1 ⁸¹Br) provides additional information if a signal detected at a certain mass contains a cluster with bromide, because similar signals need to be contained at two masses (m/z and m/z+2). Therefore, HO₂ · Br⁻ is detected on masses 112 and 114 with similar intensities. Both signals can be used for the data evaluation in order to improve the signal-to-noise ratio.

The data are analyzed using the following procedure. 30 mass spectra measured with a time resolution of 2 s are summed up to improve the signal-to-noise ratio (cf. Sect. 3.3). A mass spectrum including the mass peaks used is shown in the supplementary material. The HO₂ · Br⁻ ion cluster ion count rate (m/z 112) is normalized to the count rate of the primary ion (m/z 79). The isotopic signal at a mass-to-charge ratio of 114 and 81 are treated in the same way. The signal at both isotopic masses of the HO₂ · Br⁻ ion cluster are compared to check for possible interference from ions not containing a bromide molecule. In the following step, a water vapor dependent sensitivity is applied to convert the signal to a HO₂ concentration. Details about the water vapor dependent sensitivity are presented in Sect. 3.2. Finally a constant background is subtracted from the data. No difference in the isotopic signals was observed showing that no other molecule (not containing bromide) is interfering. In this study, only data from one of the two isotopes (m/z 112 and 79) are discussed for simplicity.

2.2 HO₂ detection by laser-induced fluorescence

The LIF instrument uses two detection channels to simultaneously detect OH and HO₂. The LIF instrument has been described in detail by Holland et al. (2003), Fuchs et al. (2011), and Tan et al. (2017).

For the HO₂ measurement, a gas stream of ambient air is expanded in to the fluorescence cell at 4 hPa. NO is added to the sampled air for the conversion of HO₂ to OH (Reaction R1). The NO concentration is adjusted to provide a HO₂ conversion efficiency of approximately 10 % in order to minimized concurrent RO₂ conversion (Fuchs et al., 2011). The OH radicals are excited by a laser pulse at 308 nm, provided by a dye laser system. Ozone can be photolysed at 308 nm, which can lead to a small interference from ozone that is subtracted from the measured signal. For the experiments discussed here, 50 ppbv O₃ gave a signal that is equivalent to an HO₂ concentration of 3 × 10⁶ cm⁻³. The sensitivity of the HO₂ LIF detection is water vapor dependent due to the quenching of the OH fluorescence by water. The change in the sensitivity is calculated from quenching constants. Both corrections are taken into account in the data presented here. The accuracy of the LIF HO₂ measurement is ±10 % from the uncertainty of the calibration. The typical precision of measurements gives an limit of detection of 1 × 10⁷ mol cm⁻³ (2σ) for a 80 s measurement (Tan et al., 2017).

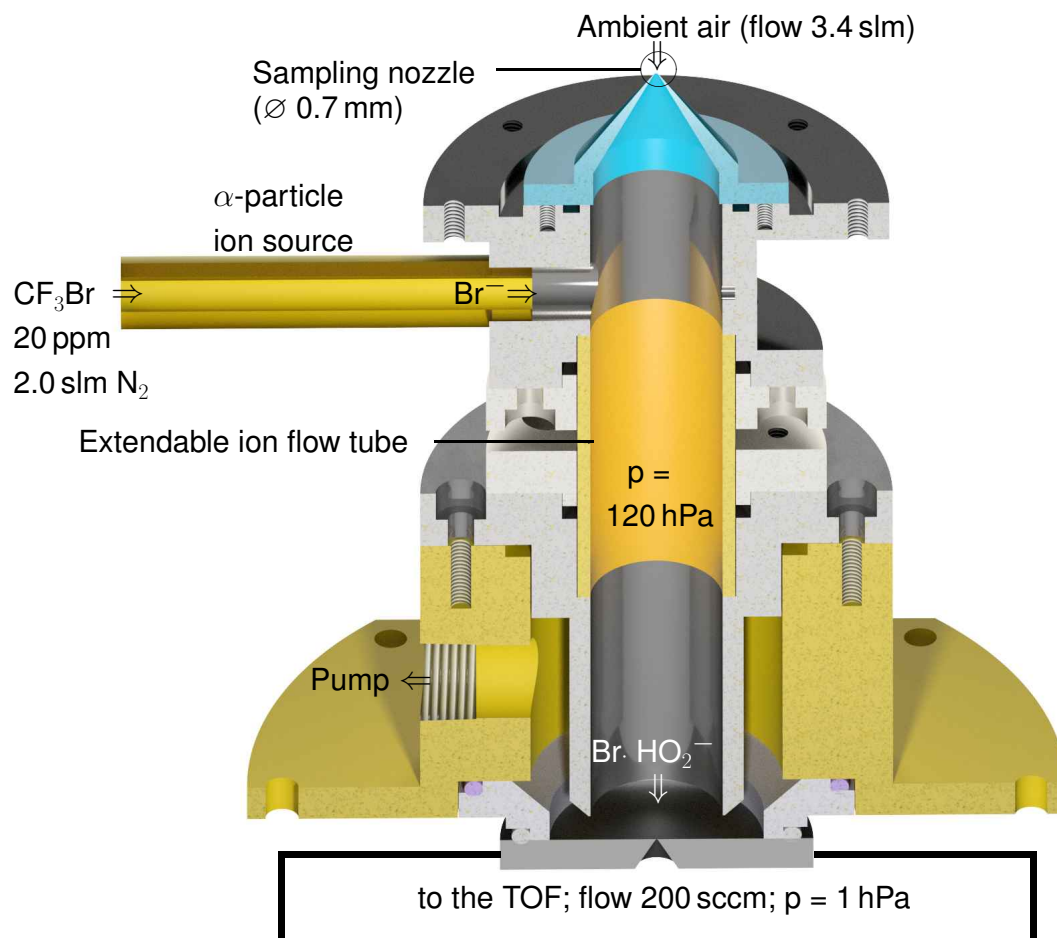


Figure 1. Schematic drawing of the ion flow tube, where HO_2 clusters with Br^- are formed. The ion flow-tube is mounted upstream of an Aerodyne Time-of-Flight mass spectrometer.

2.3 SAPHIR

SAPHIR is an atmospheric simulation chamber at Forschungszentrum Jülich. The chamber has been described in detail by Rohrer et al. (2005). It consists of a double-wall FEP film of cylindrical shape (length 18 m, diameter 5 m, volume 270 m^3). It is equipped with a shutter system that can be opened to expose the chamber air to natural sunlight. Synthetic air used in the experiments is produced from liquid nitrogen and oxygen of highest purity (Linde, purity $<99.9999\%$). A combination of sensitive measurement instruments allows for studying chemical systems under well-defined, atmospheric conditions and trace gas concentrations. SAPHIR has proven to be a valuable tool for inter-comparisons of different measurement techniques (Fuchs et al., 2012; Dorn et al., 2013; Fuchs et al., 2010; Apel et al., 2008), as it is ensured that all instruments sample the same air composition.

For this study, measurements were performed during a series of experiments in the SAPHIR chamber in May and June 2017. The focus of the experiments was to study the chemistry of two classes of oxidation products of isoprene: the isoprene hydroxyhydroperoxides (ISOPOOH) and the isoprene epoxydiols (IEPOX). In addition, reference experiments without addition of VOCs, as well as experiments with isoprene were performed. These experiments were used to compare the performance of the CIMS and the LIF instrument at atmospheric HO₂ concentrations, testing various conditions, e.g. presence of ozone, NO_x species and different water vapor concentrations.

The CIMS was mounted underneath the chamber floor, 4 m away from the LIF instrument. The ion flow tube setup shown in Fig. 1 was directly connected to the chamber, so that the sampling nozzle was sticking into the chamber.

Data from the following instruments are used for the data evaluation and interpretation: The humidity was measured using a Picarro cavity ring-down instrument (G2401 Analyzer). NO and NO₂ were monitored by a Eco Physics chemiluminescence instrument (TR780) and ozone was detected by an UV photometer (41M, Ansyco).

Measurements in the chamber were performed at daytime temperatures of roughly 20 to 30 ° Celsius. Additionally, the instrument itself was temperature stabilized to (25±5) ° Celsius to prevent temperature effects.

2.4 Calibration source

For calibrating the HO₂-CIMS instrument's sensitivity the same radical source is used as for calibration of the LIF instrument that is in operation at Forschungszentrum Jülich (Fuchs et al., 2011). This is possible because the designs of the inlet nozzle and flow rates of both instruments are similar. The LIF instrument is sampling 1.0 slm and the CIMS instrument is sampling 3.4 slm. Both flows are much smaller than the total flow through the calibration source. The calibration source provides a laminar gas stream of humidified synthetic air at a flow rate of 20 slm. The gas supply device for the calibration source allows for systematic variation of the water vapor concentration. During calibrations the water vapor concentration is altered from 0.1 to 1.6 %, in order to determine the humidity dependence of the instrument's sensitivity. Water vapor is photolysed at 185 nm at atmospheric pressure using a penray lamp leading to the production of equal concentrations of OH and HO₂ radicals (Fuchs et al., 2011). The radical concentration that is provided by the calibration source is calculated from the UV intensity that is monitored by a photo-tube detector, the flow rate and water vapor concentration. The photo-tube signal is calibrated against ozone that is concurrently produced from oxygen photolysis by the 185 nm radiation. An absorption cell in-between the UV lamp and the photolysis region can be filled with a N₂O / N₂ mixture to vary the UV intensity, as N₂O is a strong absorber at this wavelength. If excess CO is added to the synthetic air provided to the calibration source, OH is converted to HO₂, so that the HO₂ concentration is doubled compared to the operation without CO. Typically, the calibration is performed at HO₂ concentrations between 5×10^8 and 1×10^{10} molecules cm⁻³.

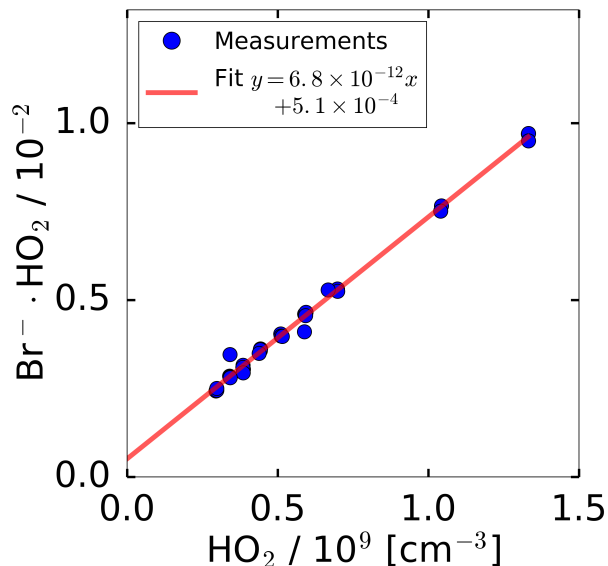


Figure 2. Count rate of $\text{HO}_2 \cdot \text{Br}^-$ ion cluster (m/z 112) normalized to the primary ion Br^- (m/z 79) during sampling from the HO_2 calibration source. The HO_2 concentration provided by the source was varied by attenuating the radiation of the 185 nm radiation used to photolyse water. The water vapor mixing ratio was kept constant. The error bars are smaller than the symbols in the figure.

3 Characterization of the HO_2 -CIMS

3.1 Linearity of measurements

In general, the conversion of ion count rates measured by a CIMS instrument to concentrations of the detected molecule requires regular calibrations of the sensitivity. For calibrating the HO_2 sensitivity, a radical source was utilized as described in Sect. 2.4. Figure 2 shows the measured, normalized ion count rates measured by the CIMS, when the calibration source was operated at a constant water vapor mixing ratio of 1.0%. The HO_2 concentration was varied by changing the UV radiation intensity by varying the N_2O concentration in the absorption cell of the calibration source. A linear behavior for the normalized count rate measured by the CIMS instrument is observed in the tested range of 3.0×10^8 to 1.3×10^9 HO_2 molecules cm^{-3} . The slope of the linear regression gives the calibration factor of $6.8 \times 10^{-12} \text{ cm}^3$. The intercept of 5.1×10^{-4} of the linear fit indicates a HO_2 background signal that was not corrected in Fig. 2.

3.2 Instrument sensitivity

The possible dependence of the HO₂ detection sensitivity on the concentration of gaseous water vapor mixing ratio was studied using two different radical sources. The water dependent calibration factor is defined by Eq. 1, where *c* represents the instrument sensitivity that depends on the water concentration.

$$5 \quad \frac{m/z(112)}{m/z(79)} = c(\text{H}_2\text{O}) * [\text{HO}_2] \quad (1)$$

One of the radical sources is described in Sect. 2.4. Keeping the UV flux of the photolysis lamp constant, different HO₂ concentrations were produced by varying the water-vapor mixing-ratio between 0.1 - 1.2%. As the HO₂ concentration provided by the calibration can be accurately calculated for different water mixing ratios, the influence of water on the HO₂ detection sensitivity could be investigated. Measurements at dry conditions were not possible, because the calibration source needs water
10 to generate HO₂.

For low water vapor concentrations, ozonolysis of 2,3 dimethyl-2-butene was used as a radical source. For that purpose, the alkene was added in a concentration of 30 ppbv to a mix of synthetic air and 200 ppbv ozone. The radical source (with photolysis lamp switched off) was used as a flow-tube to overflow the inlet of the instrument with this gas mixture. 0.2% CO was added to scavenge OH radicals produced from the ozonolysis reaction by a fast conversion of OH to HO₂. The water
15 mixing ratio was altered during the ozonolysis experiment from 0.0 to 0.6%. Assuming that the HO₂ concentration from the ozonolysis is constant, the relative change in the signal gives the relative change of the instrument sensitivity. Absolute sensitivities were derived by scaling the HO₂ signals from the ozonolysis experiment to the concentration derived by the water dependent calibration from the radical source by multiplication with a constant factor.

Figure 3 shows the sensitivity determined for each water vapor mixing ratio showing a decreasing sensitivity with increasing
20 water vapor mixing ratio for atmospheric relevant water mixing ratios higher than 0.1 %. The water dependent decrease in sensitivity is nearly linear for this range of water vapor mixing ratios. For water vapor mixing ratio of less than 0.1 %, the sensitivity drops quickly by a factor of 7 at dry conditions compared to the maximum sensitivity at 0.1 % water vapor mixing ratio.

Two effects contribute to the water dependence: The initial increase of sensitivity (below 0.1% H₂O) comes from the
25 stabilizing effect of H₂O. Br⁻ adds H₂O, forming a loosely bound complex of H₂O · Br⁻; then, the H₂O · Br⁻ complex reacts with HO₂ according to the forward reaction R2. The steady decrease of sensitivity by a factor of 2 when the H₂O mixing ratio is further increased to 1.2% comes from the back reaction of reaction R2.



The water vapor dependence of the sensitivity can be parameterized by a third order polynomial (Eq. 2) for water vapor
30 mixing ratios higher than 0.1 %. This is typically sufficient for atmospheric conditions. At lower water vapor mixing ratios

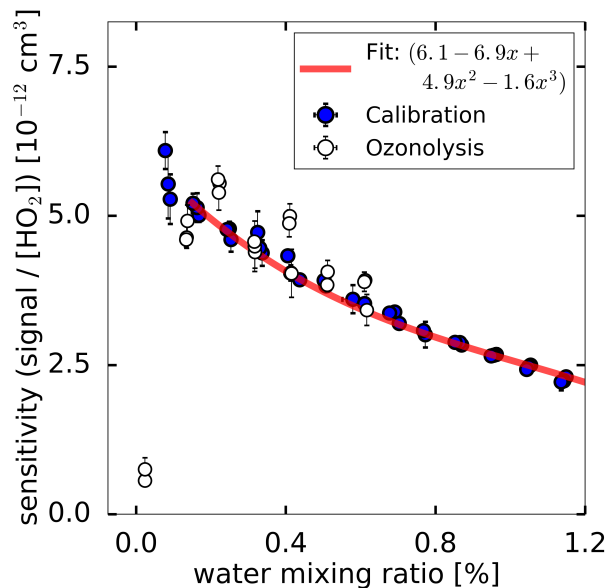


Figure 3. Measured HO₂ sensitivity as a function of the water mixing ratio in two experiments. For the calibration, HO₂ was produced by the radical source while varying the water vapor concentration which causes a change in the HO₂ radical concentration. During the ozonolysis experiment, HO₂ was produced from the ozonolysis of 2,3-dimethyl-2-butene, which is independent of the water vapor mixing ratio. The red line shows a third order polynomial fit applied to the calibration data for the range of water vapor mixing ratios higher than 0.1 %.

the parametrisation in Eq. 3 provides a good approximation. Such low water vapor mixing ratios were present in the chamber experiments after flushing the chamber before an experiment started.

$$S = a \times \text{H}_2\text{O}^3 + b \times \text{H}_2\text{O}^2 + c \times \text{H}_2\text{O} + d \quad : \quad \text{H}_2\text{O} \geq 0.1\% \quad (2)$$

$$S = c \times \text{H}_2\text{O}^{-0.4} + b \times \text{H}_2\text{O} + a \quad : \quad \text{H}_2\text{O} < 0.1\% \quad (3)$$

5 S is the signal normalized by the primary ion, a, b, c, d are the fit parameters and H₂O is the absolute water vapor mixing ratio. During the series of chamber experiments presented in Sect. 3.5, calibrations were done in-between the experiments. In the middle of the series of experiments (06 June), settings of the instrument were tuned changing the sensitivity of the instrument. In total 6 calibrations were performed.

To gain sensitivity the wall contact was reduced by directly sampling via a nozzle into the ion flow tube in the instrument here. The ion flow tube was further optimized for length and pressure to improve the sensitivity for HO₂. Basically the ion flow tube used during this study (130 mm length) was compared to a similar ion flow tube with a length of 200 mm. However, this resulted in 50 % less sensitivity at 120 hPa, which has been identified as the optimal pressure in terms of sensitivity. Finally

the flows were optimized to gain the maximum in sensitivity. Further sensitivity can be gained combining both isotopic signals for the data analysis as already mentioned by Sanchez et al. (2016).

For the chamber experiments, the chamber air was humidified at the beginning of each experiment. At that time, no HO₂ is expected to be present in the chamber. Therefore, the signal caused by the constant HO₂ background changes with the water vapor dependence of the instrument sensitivity (see next section) and could be used to determine the relative change of the sensitivity on water vapor for an individual experiment during this measurement campaign. All HO₂ data from the chamber experiments shown in Sect. 3.5 were evaluated by applying this procedure.

As shown in Fig. 3, the instrument response to the change of the water vapor concentration is similar both methods of radical production. In addition, the instrument's sensitivity at dry conditions could be tested in the ozonolysis case showing that the instrument sensitivity drops by nearly an order of magnitude in the absence of water vapor. Because of the fast drop of the instrument's sensitivity for water vapor mixing ratios below 0.1 %, it is beneficial to add water vapor to the ion flow tube at very dry conditions of the sampled air to maintain a high instrument sensitivity.

Sanchez et al. (2016) used a similar approach to calibrate their instrument via photolysis of water, but they used water mixing ratios in the pptv range to keep HO₂ concentrations in an atmospheric range. They used purified air for the calibration source. This study uses synthetic air (purity 99.9999%).

Sanchez et al. (2016) found a constant sensitivity for water vapor mixing ratios between 0.2 and 0.8% whereas a 30% decrease is observed here. Only for one sensitivity measurement at 0.06% water mixing ratios an increased sensitivity by approximately 50% is reported by Sanchez et al. (2016). The reason for this different behaviour is not clear, but one may speculate that the design of the ion-flow tube and inlet nozzle might impact the collision probability of ion clusters. The relative change of the instrument's sensitivity in Sanchez et al. (2016) towards dry conditions is not reported, so that it is not clear, if the sensitivity drops for dry conditions in their instruments as observed here.

3.3 Precision and uncertainty of the HO₂ measurement

To determine the instrument's limit of detection, the Allan deviation was calculated from 2 hours of measurements, when no HO₂ was present. The signals of both masses at which HO₂ is detected (112 and 114) were taken into account for this analysis. The background signal was equivalent to 1×10^8 molecules cm⁻³ and the count rate of the primary Br ion was 1×10^5 counts s⁻¹. The sensitivity during the measurement was 8×10^{-12} cm³ giving a count rate of 80 counts s⁻¹ (= 4800 counts min⁻¹) for the background signal. Poisson statistics predicts a noise that correlates to the square root of the counts, which fits well with the results of the Allan division plot shown in Fig. 4. This correlates to a signal with an expected noise of 70 counts that gives a 1- σ limit of detection of 0.015×10^8 molecules cm⁻³ for 60 s integration time. This is slightly better than the 1- σ level of detection of 0.06×10^8 molecules cm⁻³ reported for the instrument in Sanchez et al. (2016).

Uncertainties are caused by the calibration, which makes the major contribution of the measurement uncertainty with $\pm 10\%$ (1σ) (Holland et al., 2003). The stability of the background signal in the measurements done here was $\pm 12\%$, giving an upper limit of the additional uncertainty from the stability of the subtracted background signal. Similar uncertainties are obtained by Sanchez et al. (2016).

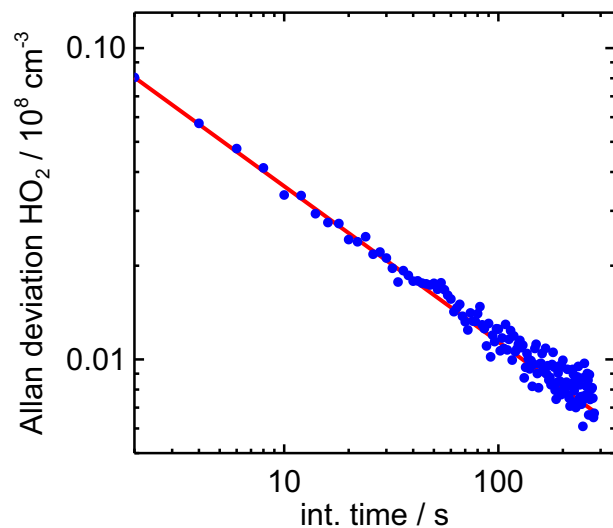


Figure 4. Allan deviation plot derived from sampling a constant HO₂ concentration of 1×10^8 HO₂ molecules cm⁻³ over 5 hours. The Allan deviation demonstrates the precision of measurements depending on the integration time. The red line indicates the behavior of the Allan deviation, if the noise is only limited by Gaussian noise.

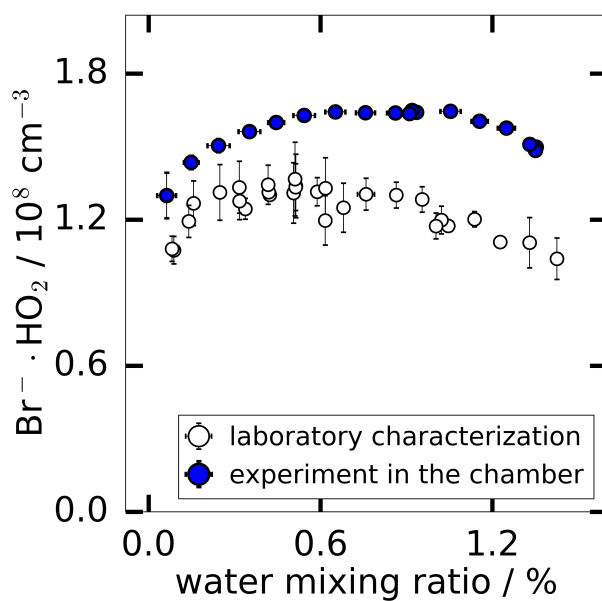


Figure 5. The background HO₂ measurement in the SAPHIR chamber derived during the humidification of the clean chamber and the background measured during the laboratory calibration supplying humidified synthetic air.

3.4 Instrumental background

The instrumental background was characterized in experiments where the inlet was overflowed with humidified synthetic air. This was done either using the radical source as a flow tube when the UV lamp was off or during experiments in SAPHIR, when only humidified synthetic air was present in the chamber. As shown in Fig. 5, the background signal changes similarly with water vapor for both experimental conditions. The shape of the water vapor dependence is consistent with the assumption that a constant HO₂ concentration ($(1.5 \pm 0.2) \times 10^8$ molecules cm⁻³) is internally produced in the instrument, which is detected according to the water vapor dependence of the instrument sensitivity discussed above. Nevertheless, Fig. 5 shows that the background was up to 20% lower in the laboratory measurement and the measured background shows a better linearity compared to the chamber measurements. Both backgrounds were calibrated using a water dependent calibration.

The background can be subtracted from the measured HO₂ concentration after applying the water vapor dependent calibration factor. The value of the background needs to be regularly determined. As reported for other CIMS instruments detecting radicals (Berresheim et al. (2000); Sanchez et al. (2016)), the radicals can be produced by the ion source. Therefore, this is the likely reason for the observed background signal. For chamber experiments reported here, the background signal was measured in the clean dark chamber at the start of each experiment. No trend of the background signal over a period of 2 month was observed. The day-to-day variability of the background (in total 16 experiments) was within a range of $\pm 12\%$ during 2 months of measurements at the chamber.

Sanchez et al. (2016) also described a constant HO₂ source which causes a background. An HO₂ titration experiment Sanchez et al. (2016) confirmed that HO₂ is internally produced, which has been discussed for other radical measurements using a CIMS approach (Berresheim et al., 2000). Sanchez et al. (2016) determined an instrument background of at least 4 pptv HO₂, which compares well with the background of 6 pptv HO₂ that has been found during the experiments in the SAPHIR chamber.

3.4.1 Potential interference from ozone

Ozone is known to be an interference in some HO₂ LIF instruments due to the photolysis of O₃ by the 308 nm excitation laser (Holland et al., 2003). In order to test whether ozone can also cause an interference in the CIMS detection of HO₂, laboratory experiments were performed. Ozone was added to humidified synthetic air (water vapor mixing ratios 0.3 and 2.6%). For both conditions no increase of the CIMS background signal could be observed for ozone mixing ratios of up to 400 ppbv. Details of the experiment are shown in the supplementary material. Results are consistent with the laboratory characterization experiments performed by Sanchez et al. (2016) for their Br- CIMS instrument.

During experiments in the SAPHIR chamber, instrument background effects can only be determined for periods of the experiments without the presence of reactants, when no HO₂ was present. A time series for a typical experiment is shown in Fig. 6. Typically, ozone was added in a concentration of 100 to 200 ppbv. Although no artefacts were found in the laboratory characterization, an increase in the background upon ozone addition was observed in two of 12 experiments in SAPHIR. For these two experiments, the chamber was first humidified and ozone was added afterwards. The increased background appears as an increased intercept of 2.3×10^8 and 1.0×10^8 HO₂ molecules cm⁻³ in the linear regression between LIF and CIMS HO₂ data for the experiments of 21 June and 26 June (Fig. 7), respectively. The data of the LIF instrument were corrected for a

maximum ozone interference of 0.05×10^8 and 0.15×10^8 HO_2 molecules cm^{-3} on these days, respectively. This correction is much smaller than the HO_2 concentration observed by the CIMS instrument, so that it can be excluded that differences are due to systematic errors in the data of the LIF instrument.

In the correlation plot (Fig. 8), including all experiments, this additional background was subtracted. The increased background due to the ozone addition will be investigated in further chamber experiments. Because no direct connection between the occurrence of this interference and chemical conditions in the experiments is observed, it might be related to instrumental effects that could vary with time such as cleanness of the ion flow tube walls. This indicates that regular checks of the background signal is needed to take an appropriate background correction into account.

3.5 Comparison of CIMS and LIF HO_2 measurements

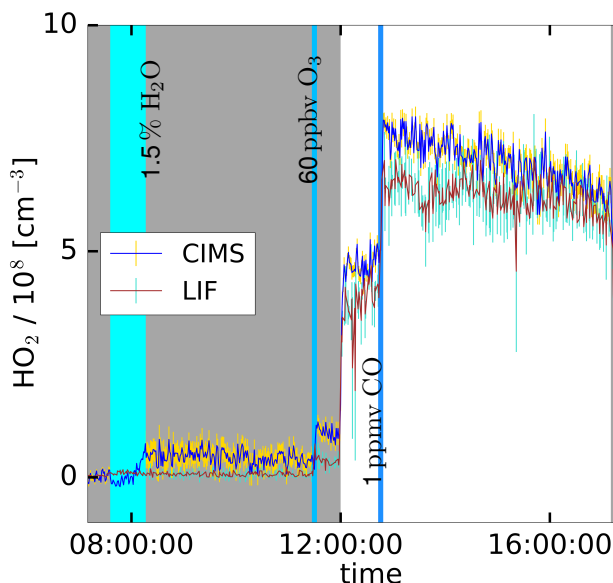


Figure 6. Time series plot for the HO_2 concentrations measured by the CIMS and the LIF instrument during the photo-oxidation experiment at 19 June 2017 in the SAPHIR chamber. The gray shaded area indicates that the chamber roof was closed. The vertical lines are showing the injection time of additional reactants, in case of water the injection took longer indicated by a broader line.

The HO_2 production was initiated with the injection of ozone and the opening of the chamber roof providing UV light to the chamber, as shown in the time series in Fig. 6. An addition of CO further boosted the HO_2 production, which dropped upon closing of the roof. After the injection of water the CIMS shows a stable signal with a small offset. During the experiment the LIF and CIMS data reveal a good correlation. This experiment was performed without the addition of a volatile organic compound (VOC), as well as, two other experiments marked with "None" in Fig. 7. Nevertheless, HO_2 is produced in these experiments, because OH and NO are produced from the photolysis of HONO released from the Teflon chamber walls in the

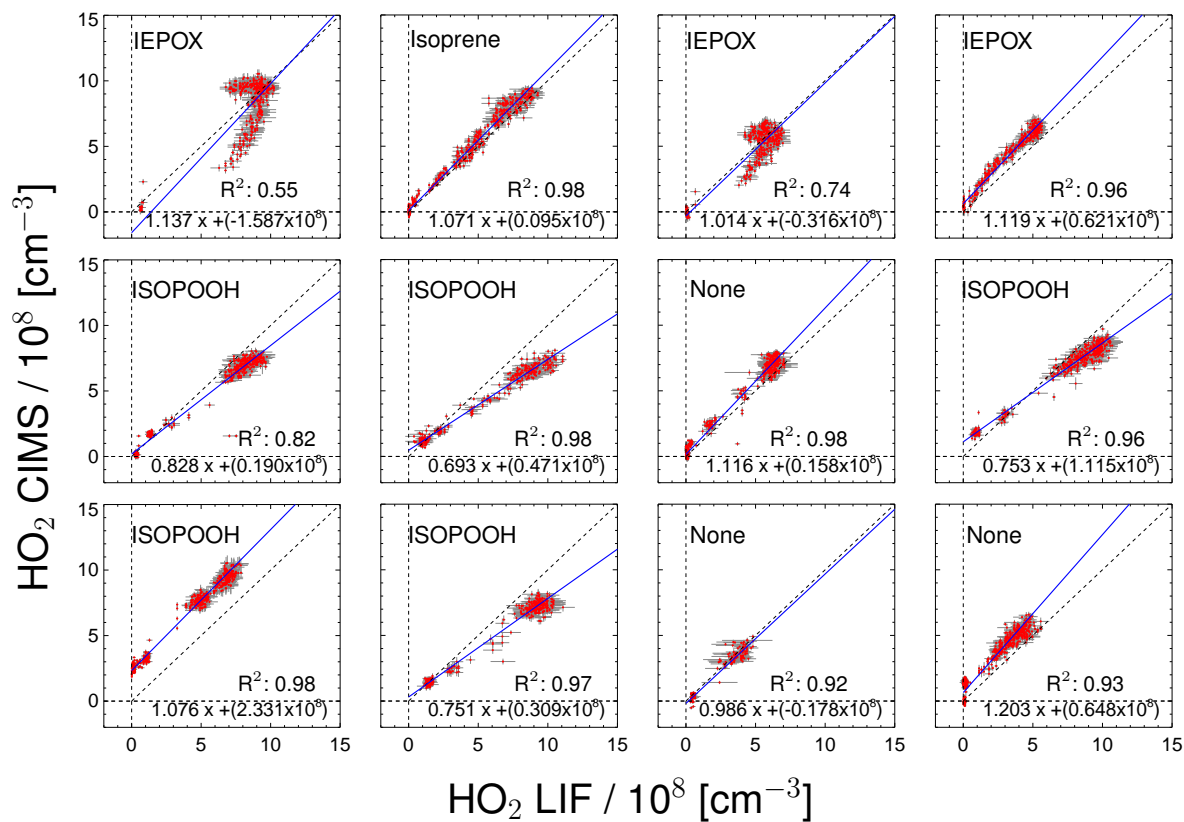


Figure 7. Correlation between HO₂ measurements by the CIMS and LIF instruments for individual chamber experiments. Labels in the plots indicate the specific VOC injected into the chamber. For the regression line shown in blue a least square fit was performed.

sunlit chamber (Rohrer et al., 2005). Reaction of small concentrations of OH reactants formed under these conditions in the chamber lead to the formation of HO₂ (Rohrer et al., 2005).

Figure 7 displays the correlation between HO₂ measurements by the CIMS and the LIF instrument for all day-long photo-oxidation experiment in the SAPHIR chamber performed in this study. The results of a linear regression analysis are given in Fig. 7, which takes errors in both HO₂ measurements into account (Press et al., 1992). The chemical composition was varied between experiments by changing for example the NO mixing ratio. The different chemical conditions during the experiments allows for checking for potential interferences. High NO concentrations of up to 3 ppbv were reached by injecting NO to the chamber air on 31 May and 02 June, and up to 80 ppbv NO₂ was added on 23 June. The NO₂ interference test was performed by injecting NO₂ in the dark, dry chamber. No further photo-chemistry experiments was done on this particular day. No systematic change in the relation between HO₂ related to the presence of NO or NO₂ from the two instruments is observed in these cases (Fig. 7), which is in agreement with the results of Sanchez et al. (2016). In general, no interference from VOCs (Isoprene, ISOPOOH and reaction products) are observed, except for experiments with IEPOX injections. IEPOX was detected on m/z 197 as Br⁻ · IEPOX ion cluster, but the instrument was not calibrated for IEPOX. Nevertheless, this mass trace

can be used to correct the HO₂ measurement for the interference from IEPOX, the correction is shown in the supplementary material. The correlation plots shown in Fig. 7 are corrected for the IEPOX interference. The HO₂ signal observed during the injection of IEPOX can be attributed to the interference from IEPOX, because IEPOX was injected in the dark chamber so that no HO₂ is expected to be present. This gives the relationship between the signal observed at the IEPOX mass (m/z 197) to the interference signal from IEPOX at the HO₂ mass (m/z 112). During the photo-oxidation of IEPOX, when also HO₂ is present, the interference signal can be subtracted from the signal at the HO₂ mass by scaling the initial interference signal by the relative change on m/z 197. The correction improves the correlation of the CIMS and the LIF but the absolute agreement is still not as good (slope of the regression 0.93; coefficient of determination 0.79) compared to the other experiments. The corrections are in the order of or smaller than the HO₂ measurements, and works best for the experiment with the lowest IEPOX concentration. A plausible reason for the IEPOX interference found seems to be a fragmentation of the cluster ion in the transfer stage of the instrument. The fragmentation could be initiated by acceleration of the ions in the electrostatic field causing collisions with other molecules. It is worth noting that IEPOX concentrations were at least 10 times higher than typically found in the atmosphere. Kaiser et al. (2016) found IEPOX concentrations of 1 ppbv during a campaign in a forest in the South-East US where isoprene, the precursor of IEPOX, was the dominant organic species. Therefore no significant interference for atmospheric measurements by the CIMS instrument are expected from IEPOX.

During experiments with ISOPOOH, HO₂ measurements by the LIF instrument showed higher values than HO₂ measured by the CIMS instrument (slope of the linear regression of 0.88; coefficient of correlation $R^2 = 0.68$). Further experiments will be needed to investigate if ISOPOOH could cause an interference in the LIF instrument. Like in the case of IEPOX, ISOPOOH concentrations were much higher (several ppbv) than typically found in the atmosphere (less than 1 ppbv Kaiser et al. (2016)), so that no significant impact for atmospheric conditions is expected.

All concurrent measurements of the two instruments for HO₂ by CIMS and LIF, in the photo-oxidation experiments are summarized in the correlation plot shown in Fig. 8. In general, the correlation fit shows that there is an excellent agreement of both instruments giving a slope of linear regression of 1.14 and the linear correlation coefficient R^2 is 0.87. Experiments investigating the photo-oxidation of IEPOX and ISOPOOH are color-coded and are excluded from the correlation fit. However, using all data for the correlation fit leads to similar result (slope of linear regression of 0.86; coefficient of correlation $R^2 = 0.89$).

Correlation of individual experiments (Fig. 7, e.g. 21 June and 26 June) give partly significant offsets in the regression analysis of up to $2.3 \times 10^8 \text{ cm}^{-3}$ HO₂. One possible reason could be the procedure, how the water vapor dependence of the instrument sensitivity was derived. This was done by using the measured signal at the HO₂ · Br⁻ mass during the humidification process of the clean chamber air, when no HO₂ was present. However, the chamber air might not be perfectly mixed during the humidification, because water vapor from boiling water is introduced at one location in the chamber together with a high flow of synthetic air. Because the water measurement in the chamber used for the determination of the CIMS background signal and the CIMS inlet are at different locations in the chamber, the water measurement is potentially not accurate for the water vapor sampled by the CIMS for these conditions, so that small systematic errors in the background determination cannot

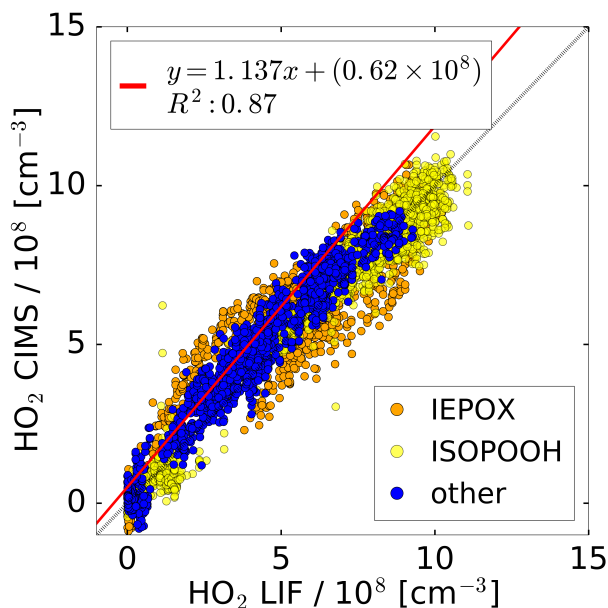


Figure 8. Correlation plot for the HO₂ concentrations measured by the CIMS and the LIF instrument of all photo-oxidation experiments in the SAPHIR chamber. A linear fit is applied to the subset of data excluding experiments with IEPOX and ISOPOOH.

be excluded. In the future, the water vapor dependence of the background will be determined independently from the chamber experiment, so that it can be expected that such effects will not be relevant.

4 Conclusion and Outlook

Chemical ionization was applied to measure atmospheric HO₂ concentrations using bromide ions as reagent. Laboratory characterization experiments and measurements in the atmospheric simulation chamber SAPHIR in Jülich were used to check the instruments applicability for atmospheric measurements.

The performance of the CIMS instrument is comparable with measurements by a laser-induced fluorescence instrument. A water vapor dependence of the instrument sensitivity needs to be taken into account in the evaluation of data because the sensitivity of the instrument changes by roughly a factor of 2 for atmospheric water vapor concentrations between 0.2 and 1.4%. Also a water vapor dependent background signal is observed. The change of the background signal with increasing water vapor, however, is explained by the water vapor dependence of the sensitivity. Therefore, the assumption is that the background consists of constant HO₂ production in the instrument. This background was stable within $\pm 12\%$ during two months of measurements and no further trend was identified. The background signal and the instrument detection sensitivity needs to be quantified on a daily basis.

No significant interference from trace gases NO, NO₂, O₃, CO, isoprene and ISOPOOH were found for atmospheric conditions. Only for non-atmospheric high IEPOX concentrations of several ppbv artificial signals were found that scaled with the

IEPOX concentration. The HO₂ measurements correlate well with the LIF measurements. A slope of the linear regression of 1.07 was determined and a linear correlation coefficient (R²) of 0.87 was found.

HO₂ was directly sampled through a nozzle into a custom-build ion flow tube which was optimized for sensitivity. The sensitivity reached is equal to 0.005 × 10⁸ HO₂ per cm³ for 10⁶ cps of bromide and 60 s of integration time, which is approximately 3 times higher than the sensitivity for a similar instrument by Sanchez et al. (2016). Therefore the instrument is suitable to measure typical HO₂ concentrations in the atmosphere. Further the Allan deviation shows that the instrument follows Gaussian noise allowing integration time of up to 500 s.

Chemical conditions in the chamber experiments were close to atmospheric conditions regarding the most important constituents of the atmosphere such as NO_x, ozone and water vapor showing the applicability of the instrument under these conditions. First future deployment in field experiments will be done with concurrent HO₂ measurements by the LIF instrument, so that potential so far unrecognized interference can be identified.

For future application of the instrument in field and chamber experiments, various modifications of the instrument will be tested to improve the sensitivity and minimized the background signal: A sheath flow of pure nitrogen in the ion flow tube could help to prevent wall contact of radicals in the ion-flow tube. Further, the sheath flow could be humidified to prevent sensitivity loss for measurements performed in dry conditions. Additionally, an automated calibration will be installed to perform daily calibration and background measurements. An important benefit of the instrument is that the bromide ion chemistry can also detect organic compounds specifically oxygenated organic compounds and acids. Therefore the technique provides a valuable tool in future field and simulation experiments.

Data availability. Data of the experiments in the SAPHIR chamber used in this work is available on the EUROCHAMP data homepage (<https://data.eurochamp.org/>, last access: June 2018).

Competing interests. The authors declare that they have no conflict of interest.

Acknowledgements. This project has received funding from the European Research Council (ERC) (SARLEP grant agreement No. 681529) and from the European Research Council(EC) under the 15 European Union's Horizon 2020 research and innovation programme (Eurochamp 2020 grant agreement No. 730997). Thanks to Patrick Veres from NOAA for discussion and first ideas regarding the HO₂ CIMS detection. We like to acknowledge Jean Rivera-Ros from the Harvard University and David Reimer from our institute for the synthesis of the VOCs used for this study. Thanks to Martin Breitenlechner, Alexander Zaytsev and Frank N. Keutsch from School of Engineering and Applied Sciences and Department of Chemistry and Chemical Biology, Harvard University, Cambridge, MA, USA for the PTR measurements performed.

References

- Andrés-Hernández, M., Stone, D., Brookes, D., Commane, R., Reeves, C., Huntrieser, H., Heard, D., Monks, P., Burrows, J., Schlager, H., et al.: Peroxy radical partitioning during the AMMA radical intercomparison exercise, *Atmos. Chem. Phys.*, 10, 10621–10638, <https://doi.org/10.5194/acpd-10-8447-2010>, 2010.
- 5 Apel, E. C., Brauers, T., Koppmann, R., Bandowe, B., Boßmeyer, J., Holzke, C., Tillmann, R., Wahner, A., Wegener, R., Brunner, A., Jocher, M., Ruuskanen, T., Spirig, C., Steigner, D., Steinbrecher, R., Gomez Alvarez, E., Müller, K., Burrows, J. P., Schade, G., Solomon, S. J., Ladstätter-Weißmayer, A., Simmonds, P., Young, D., Hopkins, J. R., Lewis, A. C., Legreid, G., Reimann, S., Hansel, A., Wisthaler, A., Blake, R. S., Ellis, A. M., Monks, P. S., and Wyche, K. P.: Intercomparison of oxygenated volatile organic compound measurements at the SAPHIR atmosphere simulation chamber, *J. Geophys. Res. Atmos.*, 113, <https://doi.org/10.1029/2008JD009865>, D20307, 2008.
- 10 Berresheim, H., Elste, T., Plass-Dülmer, C., Eiseleb, F., and Tannerb, D.: Chemical ionization mass spectrometer for long-term measurements of atmospheric OH and H₂SO₄, *International Journal of Mass Spectrometry*, 202, 91 – 109, [https://doi.org/https://doi.org/10.1016/S1387-3806\(00\)00233-5](https://doi.org/https://doi.org/10.1016/S1387-3806(00)00233-5), 2000.
- Burkert, J., Andrés-Hernández, M.-D., Stöbener, D., Burrows, J. P., Weissenmayer, M., and Kraus, A.: Peroxy radical and related trace gas measurements in the boundary layer above the Atlantic Ocean, *J. Geophys. Res. Atmos.*, 106, 5457–5477, <https://doi.org/10.1029/2000jd900613>, 2001.
- 15 Caldwell, G., Masucci, J., and Ikononou, M.: Negative ion chemical ionization mass spectrometry-binding of molecules to bromide and iodide anions, *J. Mass Spectrom.*, 24, 8–14, <https://doi.org/10.1002/oms.1210240103>, 1989.
- Cantrell, C. A., Stedman, D. H., and Wendel, G. J.: Measurement of atmospheric peroxy radicals by chemical amplification, *Anal. Chem.*, 56, 1496–1502, <https://doi.org/10.1021/ac00272a065>, 1984.
- 20 Clemitshaw, K. C., Carpenter, L. J., Penkett, S. A., and Jenkin, M. E.: A calibrated peroxy radical chemical amplifier for ground-based tropospheric measurements, *J. Geophys. Res. Atmos.*, 102, 25405–25416, <https://doi.org/10.1029/97jd01902>, 1997.
- Dorn, H.-P., Apodaca, R. L., Ball, S. M., Brauers, T., Brown, S. S., Crowley, J. N., Dubé, W. P., Fuchs, H., Häsel, R., Heitmann, U., Jones, R. L., Kiendler-Scharr, A., Labazan, I., Langridge, J. M., Meinen, J., Mentel, T. F., Platt, U., Pöhler, D., Rohrer, F., Ruth, A. A., Schlosser, E., Schuster, G., Shillings, A. J. L., Simpson, W. R., Thieser, J., Tillmann, R., Varma, R., Venables, D. S., and Wahner, A.:
- 25 Intercomparison of NO₃ radical detection instruments in the atmosphere simulation chamber SAPHIR, *Atmos. Meas. Tech.*, 6, 1111–1140, <https://doi.org/10.5194/amt-6-1111-2013>, 2013.
- Edwards, G. D., Cantrell, C. A., Stephens, S., Hill, B., Goyea, O., Shetter, R. E., Mauldin, R. L., Kosciuch, E., Tanner, D. J., and Eisele, F. L.: Chemical ionization mass spectrometer instrument for the measurement of tropospheric HO₂ and RO₂, *Anal. Chem.*, 75, 5317–5327, <https://doi.org/10.1021/ac034402b>, 2003.
- 30 Fuchs, H., Brauers, T., Dorn, H.-P., Harder, H., Häsel, R., Hofzumahaus, A., Holland, F., Kanaya, Y., Kajii, Y., Kubistin, D., Lou, S., Martinez, M., Miyamoto, K., Nishida, S., Rudolf, M., Schlosser, E., Wahner, A., Yoshino, A., and Schurath, U.: Technical Note: Formal blind intercomparison of HO₂ measurements in the atmosphere simulation chamber SAPHIR during the HO_xComp campaign, *Atmos. Chem. Phys.*, 10, 12233–12250, <https://doi.org/10.5194/acp-10-12233-2010>, 2010.
- Fuchs, H., Bohn, B., Hofzumahaus, A., Holland, F., Lu, K., Nehr, S., Rohrer, F., and Wahner, A.: Detection of HO₂ by laser-induced fluorescence: calibration and interferences from RO₂ radicals, *Atmos. Meas. Tech.*, 4, 1209, <https://doi.org/10.5194/amt-4-1209-2011>, 2011.
- 35

- Fuchs, H., Dorn, H.-P., Bachner, M., Bohn, B., Brauers, T., Gomm, S., Hofzumahaus, A., Holland, F., Nehr, S., Rohrer, F., Tillmann, R., and Wahner, A.: Comparison of OH concentration measurements by DOAS and LIF during SAPHIR chamber experiments at high OH reactivity and low NO concentration, *Atmos. Meas. Tech.*, 5, 1611–1626, <https://doi.org/10.5194/amt-5-1611-2012>, 2012.
- Green, T. J., Reeves, C. E., Fleming, Z. L., Brough, N., Rickard, A. R., Bandy, B. J., Monks, P. S., and Penkett, S. A.: An improved dual channel PERCA instrument for atmospheric measurements of peroxy radicals, *J. Environ. Monitor.*, 8, 530–536, <https://doi.org/10.1039/b514630e>, 2006.
- Hanke, M., Uecker, J., Reiner, T., and Arnold, F.: Atmospheric peroxy radicals: ROXMAS, a new mass-spectrometric methodology for speciated measurements of HO₂ and RO₂ and first results, *Int. J. Mass Spectrom.*, 213, 91–99, [https://doi.org/10.1016/S1387-3806\(01\)00548-6](https://doi.org/10.1016/S1387-3806(01)00548-6), 2002.
- 10 Harrison, A. G.: Chemical ionization mass spectrometry, CRC press, Boca Raton, 2nd edn., <https://doi.org/10.1006/rwsp.2000.0357>, 1992.
- Hastie, D. R., Weissenmayer, M., Burrows, J. P., and Harris, G. W.: Calibrated chemical amplifier for atmospheric RO_x measurements, *Anal. Chem.*, 63, 2048–2057, <https://doi.org/10.1021/ac00018a029>, 1991.
- Holland, F., Hofzumahaus, A., Schäfer, J., Kraus, A., and Pätz, H.-W.: Measurements of OH and HO₂ radical concentrations and photolysis frequencies during BERLIOZ, *J. Geophys. Res. Atmos.*, 108, <https://doi.org/10.1029/2001jd001393>, 2003.
- 15 Hornbrook, R. S., Crawford, J. H., Edwards, G. D., Goyea, O., Mauldin III, R. L., Olson, J. S., and Cantrell, C. A.: Measurements of tropospheric HO₂ and RO₂ by oxygen dilution modulation and chemical ionization mass spectrometry, *Atmos. Meas. Tech.*, 4, 735–756, <https://doi.org/10.5194/amt-4-735-2011>, 2011.
- Kaiser, J., Skog, K. M., Baumann, K., Bertman, S. B., Brown, S. B., Brune, W. H., Crouse, J. D., de Gouw, J. A., Edgerton, E. S., Feiner, P. A., Goldstein, A. H., Koss, A., Misztal, P. K., Nguyen, T. B., Olson, K. F., St. Clair, J. M., Teng, A. P., Toma, S., Wennberg, P. O., Wild, R. J., Zhang, L., and Keutsch, F. N.: Speciation of OH reactivity above the canopy of an isoprene-dominated forest, *Atmos. Chem. Phys.*, 16, 9349–9359, <https://doi.org/10.5194/acp-16-9349-2016>, 2016.
- 20 Lew, M. M., Dusanter, S., and Stevens, P. S.: Measurement of interferences associated with the detection of the hydroperoxy radical in the atmosphere using laser-induced fluorescence, *Atmos. Meas. Tech.*, 11, 95–108, <https://doi.org/10.5194/amt-11-95-2018>, 2018.
- Mihele, C. M. and Hastie, D. R.: Optimized Operation and Calibration Procedures for Radical Amplifier-Type Detectors, *J. Atmos. Ocean. Tech.*, 17, 788–794, [https://doi.org/10.1175/1520-0426\(2000\)017<0788:OOACPF>2.0.CO;2](https://doi.org/10.1175/1520-0426(2000)017<0788:OOACPF>2.0.CO;2), 2000.
- 25 Press, W. H., Teukolsky, S. A., Vetterling, W. T., and Flannery, B. P.: Numerical recipes in C, Cambridge Univ. Press, 2nd edn., 1992.
- Reiner, T., Hanke, M., and Arnold, F.: Atmospheric peroxy radical measurements by ion molecule reaction mass spectrometry: A novel analytical method using amplifying chemical conversion to sulfuric acid, *J. Geophys. Res. Atmos.*, 102, 1311–1326, <https://doi.org/10.1029/96JD02963>, 1997.
- 30 Rohrer, F., Bohn, B., Brauers, T., Brüning, D., Johnen, F.-J., Wahner, A., and Kleffmann, J.: Characterisation of the photolytic HONO-source in the atmosphere simulation chamber SAPHIR, *Atmos. Chem. Phys.*, 5, 2189–2201, <https://doi.org/10.5194/acp-5-2189-2005>, 2005.
- Sadanaga, Y., Matsumoto, J., Sakurai, K.-i., Isozaki, R., Kato, S., Nomaguchi, T., Bandow, H., and Kajii, Y.: Development of a measurement system of peroxy radicals using a chemical amplification/laser-induced fluorescence technique, *Rev. Sci. Instrum.*, 75, 864–872, <https://doi.org/10.1063/1.1666985>, 2004.
- 35 Sanchez, J., Tanner, D. J., Chen, D., Huey, L. G., and Ng, N. L.: A new technique for the direct detection of HO₂ radicals using bromide chemical ionization mass spectrometry (Br-CIMS): initial characterization, *Atmos. Meas. Tech.*, 9, 3851–3861, <https://doi.org/10.5194/amt-2016-117>, 2016.

- Tan, Z., Fuchs, H., Lu, K., Hofzumahaus, A., Bohn, B., Broch, S., Dong, H., Gomm, S., Häsel, R., He, L., Holland, F., Li, X., Liu, Y., Lu, S., Rohrer, F., Shao, M., Wang, B., Wang, M., Wu, Y., Zeng, L., Zhang, Y., Wahner, A., and Zhang, Y.: Radical chemistry at a rural site (Wangdu) in the North China Plain: observation and model calculations of OH, HO₂ and RO₂ radicals, *Atmos. Chem. Phys.*, 17, 663–690, <https://doi.org/10.5194/acp-17-663-2017>, 2017.
- 5 Veres, P., Roberts, J., Wild, R., Edwards, P., Brown, S., Bates, T., Quinn, P., Johnson, J., Zamora, R., and de Gouw, J.: Peroxynitric acid (HO₂NO₂) measurements during the UBWOS 2013 and 2014 studies using iodide ion chemical ionization mass spectrometry, *Atmos. Chem. Phys.*, 15, 8101–8114, <https://doi.org/10.5194/acpd-15-3629-2015>, 2015.
- Whalley, L. K., Blitz, M. A., Desservettaz, M., Seakins, P. W., and Heard, D. E.: Reporting the sensitivity of laser-induced fluorescence instruments used for HO₂ detection to an interference from RO₂ radicals and introducing a novel approach that enables HO₂ and certain
- 10 RO₂ types to be selectively measured, *Atmos. Meas. Tech.*, 6, 3425–3440, <https://doi.org/10.5194/amt-6-3425-2013>, 2013.
- Wood, E. C., Deming, B. L., and Kundu, S.: Ethane-based chemical amplification measurement technique for atmospheric peroxy radicals, *Environ. Sci. Technol. Lett.*, 4, 15–19, <https://doi.org/10.1021/acs.estlett.6b00438>, 2017.